Reduction in coherent phonon lifetime in Bi_2Te_3/Sb_2Te_3 superlattices

Yaguo Wang,[1] Xianfan Xu,[1,a)] and Rama Venkatasubramanian[2]
[1]*School of Mechanical Engineering and Birck Nanotechnology Center, Purdue University, West Lafayette, Indiana 47907, USA*
[2]*Center for Solid State Energetics, RTI International, Research Triangle Park, North Carolina 27709, USA*

(Received 7 July 2008; accepted 28 August 2008; published online 19 September 2008)

Femtosecond pulses are used to excite A_{1g} optical phonons in Bi_2Te_3, Sb_2Te_3, and Bi_2Te_3/Sb_2Te_3 superlattice. Time-resolved reflectivity measurements show both the low-frequency and high-frequency components of A_{1g} phonon modes. By comparing the phonon lifetime, it is found that the scattering rate (inverse of lifetime) in superlattice is significantly higher than those in Bi_2Te_3 and Sb_2Te_3. This represents the direct measurement of coherent phonon lifetime reduction in superlattice structures, consistent with the observed reduction in thermal conductivity in superlattices. © *2008 American Institute of Physics*. [DOI: 10.1063/1.2987518]

Ultrafast time-resolved optical measurement is a powerful technique to generate and detect coherent phonons.[1–3] In absorbing materials, coherent phonon is generated through a displacive excitation of coherent phonon process,[3] which was shown to be a special case of impulsive stimulated Raman scattering.[4,5] In this study, we investigated coherent phonons in V_2VI_3 compounds (V=Bi,Sb; VI=Se,Te), Bi_2Te_3 and Sb_2Te_3, which are narrow band-gap semiconductors. These materials are used as thermoelectric materials partly due to their low thermal conductivity.[6] Recently, it was found that thermal conductivity in Bi_2Te_3/Sb_2Te_3 superlattice structure is greatly reduced, even compared to its corresponding alloy, in the cross-plane direction.[7] A fundamental understanding of thermal conductivity reduction in the Bi_2Te_3/Sb_2Te_3 superlattice structure is important due to its enhanced thermoelectric figure of merit.[8] It has been suggested that the thermal conductivity reduction results from interface scattering of phonons[9,10] as well as other processes.[7] Even so, there has been no documented evidence of reduction in phonon lifetimes, coherent or otherwise, that would begin to substantiate the basis of such thermal conductivity reduction in nanoscale structures. In this letter, we present ultrafast time-resolved measurements of coherent optical phonons in Bi_2Te_3, Sb_2Te_3, and Bi_2Te_3/Sb_2Te_3 superlattice, with the aim to reveal coherent phonon lifetimes in the superlattice. Ultimately, acoustic phonons need to be characterized and correlated with the thermal transport properties. Measurement of acoustic phonons in superlattice is possible since the zone-folded acoustic phonons can be optically excited.[11]

All the experiments were performed in a standard collinear two-color (400 and 800 nm) pump-probe scheme. Laser pulses with 50 fs full width at half maximum are generated by an ultrafast laser system with the center wavelength at 800 nm, a repetition rate of 1 kHz, and a maximum pulse energy about 1 mJ. A second harmonic crystal is used to generate the pump pulses centered at 400 nm. The pump and probe beams are focused onto the sample at normal direction with diameters of 80 and 20 μm, respectively. The fluence of probe beam is around 0.02 mJ/cm^2.

a)Tel.: 1-765-494-5639. FAX: 1-765-494-0539. Electronic mail: xxu@ecn.purdue.edu.

Samples investigated in this paper are *p*-type single crystalline Bi_2Te_3 film, Sb_2Te_3 film, and Bi_2Te_3/Sb_2Te_3 superlattice, with thicknesses of 1.0, 1.6, and 1.3 μm, respectively. All these films are much thicker than their absorption depth (tens of nanometers) at 800 and 400 nm laser wavelengths. The films were grown by the metal-organic chemical-vapor deposition technique on GaAs(100) substrates along the *c* axis of the films.[12] The superlattice has 200 periods with a 2 nm Bi_2Te_3 layer and a 4 nm Sb_2Te_3 layer for each period. A 150 nm Bi_2Te_3 buffer layer exists between the superlattice and the substrate. These 2 nm/4 nm Bi_2Te_3/Sb_2Te_3 superlattices show strong satellites in x-ray diffraction studies, negligible static disorder as measured by x-ray absorption spectroscopy, and also show high thermoelectric figure of merit.

Figure 1 shows time-resolved reflectivity signals at a number of pump fluences and their Fourier transforms. The experimental data consist of the following two components: the oscillatory components, which are the coherent phonon vibration, and the nonoscillatory components, which are related to electron excitation (initial drop in reflectivity) and lattice heating due to electron-lattice coupling (the second drop around 10 ps or so).[13] One observation from Figs. 1(b), 1(d), and 1(f) is the two frequency components of coherent phonon vibration for each sample, corresponding to the two A_{1g} modes (a low-frequency component—A_{1g}^1 mode and a high-frequency component—A_{1g}^2 mode). These modes were also observed in Raman scattering experiments,[14] but have not been reported in any previous time-domain experiments in literature. Table I summarizes the results from both Raman scattering and pump-probe experiment. It is seen that the vibration frequencies of the low and high-frequency A_{1g} modes for both Bi_2Te_3 and Sb_2Te_3 samples agree well with the Raman measurement results carried out in their respective bulk materials. The two modes observed in the superlattice are very close to that in Sb_2Te_3 (Raman data are not available for the bulk superlattices from literature). That is, we did not observe frequency of Bi_2Te_3—the coherent phonon modes of Bi_2Te_3 could be suppressed or dissipate at a much faster rate (see discussions below).

The oscillatory and nonoscillatory components can be separated by applying a digital low-pass filter on the experimental data. The signal of coherent phonon for all the samples, shown in Fig. 2, are obtained by filtering the nonoscillatory component. The reflectivity change ($\Delta R/R$)

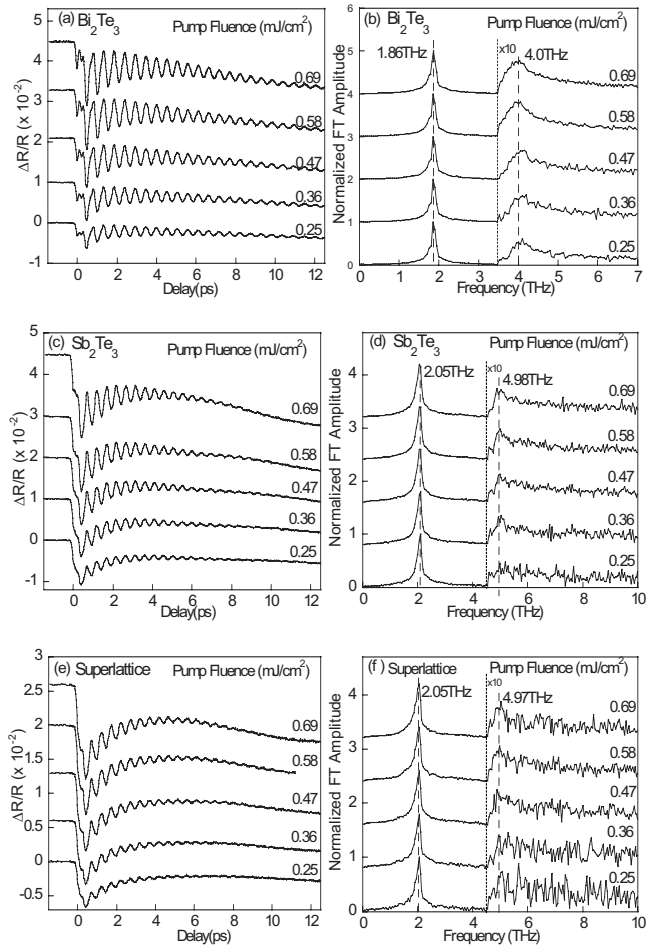

FIG. 1. [(a), (c), and (e)] Reflectivity change for Bi_2Te_3, Sb_2Te_3, and Bi_2Te_3/Sb_2Te_3 superlattice at different pump fluences. [(b), (d). and (f)] The corresponding frequency spectrum calculated by FFT. Part of the spectrum curves are magnified ten times to see the A_{1g}^2 mode clearly. All the curves are vertically translated and labeled with the pump fluence.

due to the coherent phonon can be approximated as

$$\frac{\Delta R}{R} = \frac{\partial(\Delta R/R)}{\partial Q} Q = \frac{\partial(\Delta R/R)}{\partial Q} A Q_0, \tag{1}$$

where A is the amplitude of coherent phonon vibration and Q_0 is the normalized coordinate of coherent phonon. Q_0 can be modeled as a chirped damping harmonic oscillator:[13,15,16]

$$Q_0 = \exp(-\Gamma t)\cos[(\Omega + \beta t)t + \varphi], \tag{2}$$

where Γ, Ω, β, φ are phonon scattering rate, angular frequency, chirping coefficient, and initial phase of phonon vibration, respectively. Since the vibration for the A_{1g}^2 mode is much weaker and decades much faster than the A_{1g}^1 mode, its contribution in the fitting process is negligible. Therefore, in the model and the discussion below, we only consider the contribution from the A_{1g}^1 mode.

TABLE I. Comparison of A_{1g} phonon frequencies from Raman scattering and pump-probe experiment

	Bi_2Te_3		Sb_2Te_3		Superlattice	
	Frequency (THz)		Frequency (THz)		Frequency (THz)	
Mode	Raman	Pump-probe	Raman	Pump-probe	Raman	Pump-probe
A_{1g}^1	1.88	1.86	2.07	2.05	···	2.05
A_{1g}^2	4.02	4.00	4.95	4.98	···	4.97

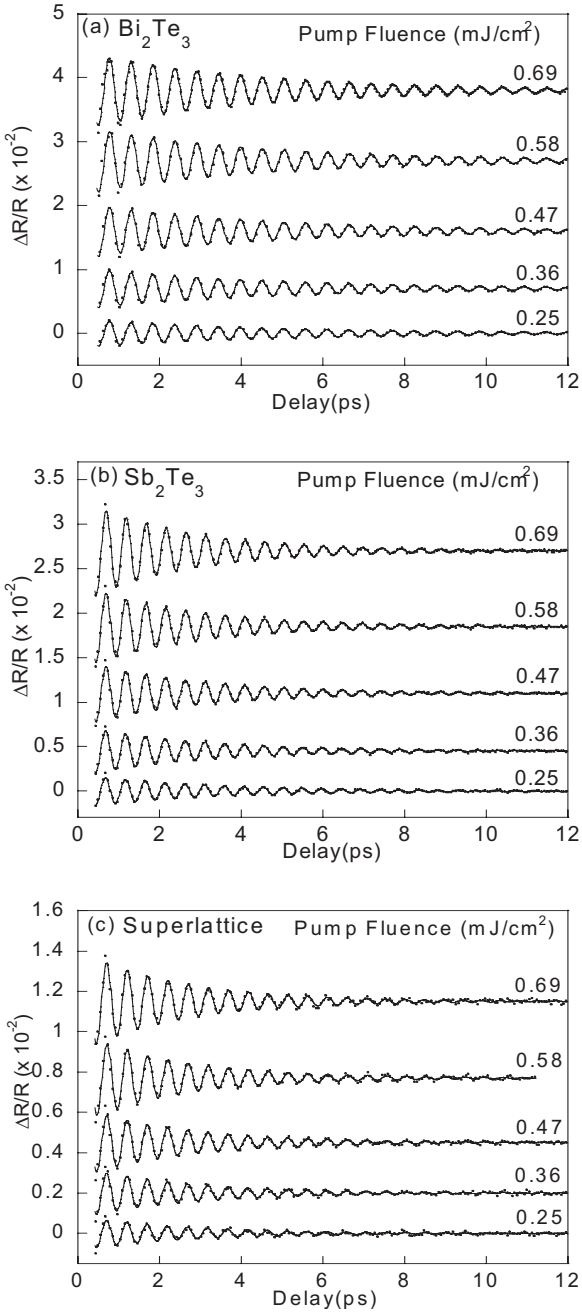

FIG. 2. Coherent phonon vibration signal for Bi_2Te_3, Sb_2Te_3, and Bi_2Te_3/Sb_2Te_3 superlattice. The dots are experimental data, and lines are fitted results.

One observation from Fig. 2 is that at the same laser fluence, the initial amplitudes of coherent phonon oscillations in the superlattice are a factor of 2–3 smaller than those in either Bi_2Te_3 or Sb_2Te_3 films. On the other hand, it is seen from Fig. 1 that the initial electron excitation (the initial reflectivity drop) for all samples, including the superlattice are close at the same laser fluence, indicating that the laser energies absorbed by the two components as well by the superlattice are similar. Therefore, the weaker phonon oscillation in the superlattice could be caused by a weaker coupling between electrons and the lattice in Bi_2Te_3 or by rapid quenching of coherent phonons in Bi_2Te_3 in a superlattice structure, which are supported by the phonon frequency measurement. The weaker electron-lattice coupling could also be

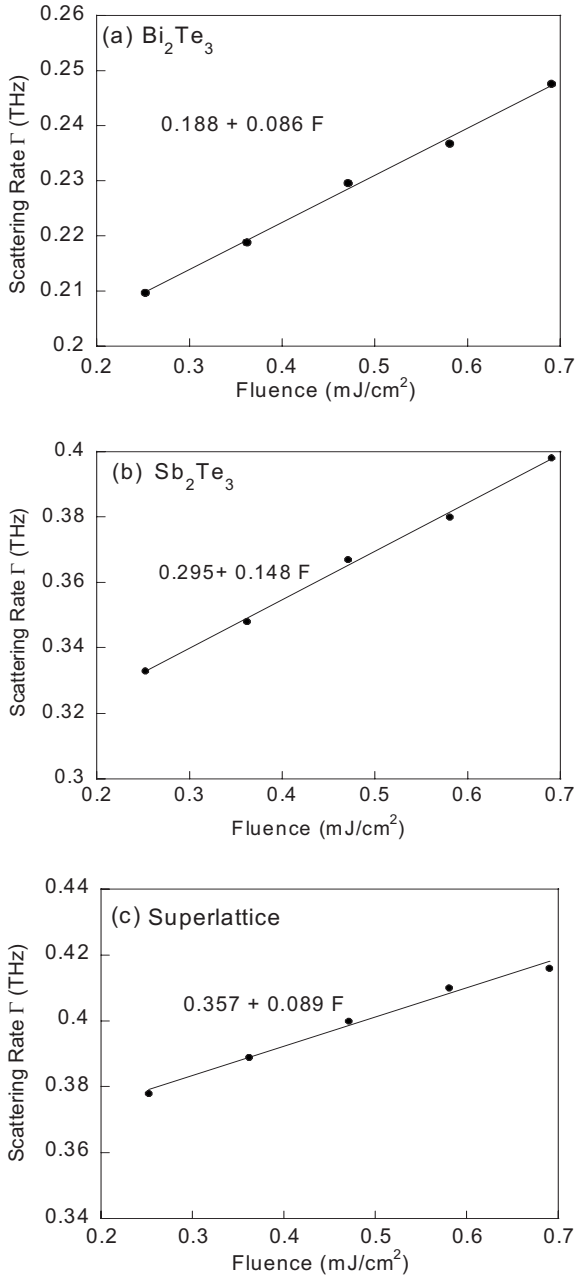

FIG. 3. Scattering rate of A_{1g}^1 mode with different pump fluences. The dots are experimental data, and the lines are fitted results.

aided by the electrons and holes, forming a miniband in a superlattice.[8] In any case, the absence of coherent phonons from the minority component of the superlattice and the overall initial amplitude are telling of interesting physical phenomena that warrant further investigations.

The phonon scattering rate—the inverse of coherent phonon dephasing time fitted from Eq. (2)—has a linear dependence on the pump fluence, as shown in Fig. 3. At higher laser fluences, photoexcited electrons contribute to the process of shortening coherent phonon lifetime or increasing the scattering. After photon excitation, the excited electrons release their excess kinetic energy by emitting incoherent phonons. Both the photoexcited electrons and the resulting incoherent phonons have a linear dependence on pump fluence, which results in the linear dependence of scattering rate on pump fluence. If the linear relation between the pump fluence and the scattering rate is extrapolated to the zero pump fluence, the phonon scattering rate under no excitation condition (Γ_0) is obtained. These scattering rates for Bi_2Te_3, Sb_2Te_3, and Bi_2Te_3/Sb_2Te_3 superlattice are found to be 0.188, 0.295, and 0.357 THz, respectively. Apparently, the scattering rate of the superlattice is higher than any of its components, 90% higher than that in Bi_2Te_3 and 20% higher than that in Sb_2Te_3. This result supports the existence of extra phonon lifetime reduction in superlattice, which may stem from a variety of scattering processes at the interfaces between the constituent layers of the superlattice. If such behaviors also exist for acoustic phonons, particularly the long wavelength acoustic phonons that have similar small wave vector as the optical phonons, that would explain the reduction in heat transport in superlattice.

In conclusion, we observed both the low-frequency and high-frequency components of A_{1g} phonon in Bi_2Te_3, Sb_2Te_3, and Bi_2Te_3/Sb_2Te_3 superlattice. The coherent optical phonon lifetime in the superlattice is shorter than those in Bi_2Te_3 and Sb_2Te_3; and the phonon vibration modes in superlattice are very similar to those in Sb_2Te_3. The phonon lifetime reduction in superlattice suggests phonon-interface interactions. This could form the basis for phonon-blocking and electron-transmitting characteristics of the superlattices.[8] Further studies are needed to elucidate the nature and mechanism of such enhanced scattering processes in a variety of nanoscale materials.

We would like to acknowledge the support to this work by the National Science Foundation, the Sandia National Laboratory, and the Air Force Office of Scientific Research. The work at RTI International was carried out with DARPA/DSO funded efforts, ONR U.S. Navy Contract No. N00014-04-C-0042 and ARO U.S. ARMY Contract No. W911NF-08-C-0058. These program supports are gratefully acknowledged.

[1] T. K. Cheng, S. D. Brorson, A. S. Kazeroonian, J. S. Moodera, G. Dresselhaus, M. S. Dresselhaus, and E. P. Ippen, Appl. Phys. Lett. **57**, 1004 (1990).
[2] T. K. Cheng, J. Vidal, H. J. Zeiger, G. Dresselhaus, M. S. Dresselhaus, and E. P. Ippen, Appl. Phys. Lett. **59**, 1923 (1991).
[3] H. J. Zeiger, J. Vidal, T. K. Cheng, E. P. Ippen, G. Dresselhaus, and M. S. Dresselhaus, Phys. Rev. B **45**, 768 (1992).
[4] G. A. Garrett, T. F. Albrecht, J. F. Whitaker, and R. Merlin, Phys. Rev. Lett. **77**, 3661 (1996).
[5] T. E. Stevens, J. Kuhl, and R. Merlin, Phys. Rev. B **65**, 144304 (2002).
[6] F. J. DiSalvo, Science **285**, 703 (1999).
[7] R. Venkatasubramanian, Phys. Rev. B **61**, 3091 (2000).
[8] R. Venkatasubramanian, E. Siivola, T. Colpitts, and B. O'Quinn, Nature (London) **413**, 597 (2001).
[9] G. Chen, Phys. Rev. B **57**, 14958 (1998).
[10] M. N. Touzelbaev, P. Zhou, R. Venkatasubramanian, and K. E. Goodson, J. Appl. Phys. **90**, 763 (2001).
[11] T. Dekorsy, A. Bartels, H. Kurz, K. Mizoguchi, M. Nakayama, and K. Köhler, Phys. Status Solidi B **215**, 425 (1999).
[12] R. Venkatasubramanian, T. Colpitts, E. Watko, M. Lamvik, and N. ElMasry, J. Cryst. Growth **170**, 817 (1997).
[13] A. Q. Wu and X. Xu, Appl. Phys. Lett. **90**, 251111 (2007).
[14] W. Richter, H. Köhler, and C. R. Becker, Phys. Status Solidi B **84**, 619 (1977).
[15] O. V. Misochko, M. Hase, K. Ishioka, and M. Kitajima, Phys. Rev. Lett. **92**, 197401 (2004).
[16] A. Q. Wu, X. Xu, and R. Venkatasubramanian, Appl. Phys. Lett. **92**, 011108 (2008).